

The Large Peculiar Velocity of the cD Galaxy in Abell 3653

Kevin A. Pimblet^{1,2}, Isaac G. Roseboom¹, Marianne T. Doyle¹

¹*Department of Physics, University of Queensland, Brisbane, 4072 Queensland, Australia*

²*email: pimblet@physics.uq.edu.au*

DRAFT: 3 SEPTEMBER 2018 — DO NOT DISTRIBUTE

ABSTRACT

We present a catalogue of galaxies in Abell 3653 from observations made with the 2dF spectrograph at the Anglo-Australian Telescope. Of the 391 objects observed, we find 111 are bone-fide members of Abell 3653. We show that the cluster has a velocity of $cz = 32214 \pm 83 \text{ kms}^{-1}$ ($z = 0.10738 \pm 0.00027$), with a velocity dispersion typical of rich, massive clusters of $\sigma_{cz} = 880^{+66}_{-54}$. We find that the cD galaxy has a peculiar velocity of $683 \pm 96 \text{ kms}^{-1}$ in the cluster restframe – some 7σ away from the mean cluster velocity, making it one of the largest and most significant peculiar velocities found for a cD galaxy to date. We investigate the cluster for signs of substructure, but do not find any significant groupings on any length scale. We consider the implications of our findings on cD formation theories.

Key words: surveys – catalogues – galaxies: clusters: individual: Abell 3653 – galaxies: elliptical and lenticular, cD – galaxies: kinematics and dynamics

1 INTRODUCTION

Clusters of galaxies permit the study of a large number of galaxies ($\sim 10^3$) at a common distance (likely co-eval) – this makes them ideal laboratories for studying galaxy evolution. They generally feature predominantly early-type (elliptical and lenticular) galaxies in their core regions, often with a central cD galaxy in residence. cD galaxies are an extreme example of giant ellipticals: they are surrounded by a low surface brightness envelope and are only ever found in groups or clusters: never in isolation in field (i.e. low density) environs. The formation mechanism(s) for cD galaxies has been hotly debated in the literature for some time.

The formation of a central cluster galaxy may be explicitly associated with the post-virialization accretion of smaller mass galaxies by the central galaxy. This process, devised by Ostriker & Tremaine (1975), is aptly known as galactic cannibalism (see also Nipoti et al. 2004; 2003; Garijo, Athanassoula, & Garcia-Gomez 1997; Blakeslee & Tonry 1992; Capelato et al. 1985; Duncan, Farouki, & Shapiro 1983; Hausman & Ostriker 1978). The theory predicts that we must be able to observe the process happening: multiple cores of cD and D galaxies in clusters should be visible. Indeed, it is the case that many cD galaxies are found to have multiple nuclei (e.g. Yamada et al. 2002; Gregorini et al. 1994; Blakeslee & Tonry 1992; Merrifield & Kent 1991; Lauer 1988).

It is possible at higher redshifts to see the progenitors of cD galaxies as multiple cluster galaxies coming together. Yamada et al. (2002) shows that the brightest cluster galaxy in

a cluster at $z = 1.26$ is composed of two distinct sub-units that are likely to fully merge on a timescale of 10^8 years. Their result is broadly in agreement with numerical predictions that show central galaxies grow through repeated mergers of smaller mass galaxies (e.g. Dubinski 1998; Garijo et al. 1997).

However, for the cD galaxy to attain enough mass and luminosity to account for these observations, it must be preferentially situated at the cluster centre where the cannibalistic accretion process is at peak efficiency (Barnes & Hernquist 1992; Tremaine 1990). Indeed, in such a post-virialization formation model of cD galaxies, dynamical friction between the inter-galactic medium and the cluster galaxies will cause the larger cluster galaxies to fall to the centre of a cluster and eventually merge with the cD galaxy that is already there.

Galactic cannibalism cannot be such a strong driving mechanism, though. Lauer (1988) shows that cannibalism cannot account for the large observed luminosities of cD galaxies. Another problem that Merritt (1985) points out with this scenario is that galaxy halos will be disrupted by the tidal field of a cluster. This leads directly to the dynamical friction timescale being increased and hence the effect of galactic cannibalism will be decreased significantly. Merritt (1984) and Smith et al. (1985) also suggest that the majority of multiple-nucleus systems are transient phenomena, and are not galaxies in the process of merging.

As an alternative to the post-virialization formation of cD galaxies, Merritt (1985; 1984) suggests that they could form before or during the virialization of rich clusters. More-

arXiv:astro-ph/0602106v1 6 Feb 2006

over, cD galaxies must also form at roughly the dynamical centre of the cluster to avoid having its outer envelope truncated by tidal forces. Many observations confirm that cD galaxies are located at the dynamic centres of galaxy clusters (e.g. Oegerle & Hill 2001; Quintana & Lawrie 1982). However, if clusters grow hierarchically through repeated mergers of sub-clusters and galaxy groups, then presumably the cD galaxy would have already been formed in one of these sub-clusters before drifting to the centre of the cluster.

This would yield two observable ‘smoking-guns’. The first would be the presence of substructure in a cluster meaning that the cluster is a dynamically young entity. The second would be a high peculiar velocity of the cD galaxy with respect to the parent cluster. We note that these two quantities are related. Oegerle & Hill (2001) show that substructure can account for, and perhaps even drive, cD peculiar velocities. Indeed, a cD galaxy may even be considered as a road-sign to substructure (Zabludoff et al. 1993; Beers & Geller 1983).

Malumuth (1992) explores if it is possible to form cD galaxies with large residual peculiar velocities in N-body simulations of cluster formation and growth. These simulations not only include the effect of dynamical friction and two body relaxation, but also comprise the role of galaxy-galaxy stripping collisions and mergers. Within $\sim 10^{10}$ years, Malumuth (1992) shows that the cD galaxies in the simulations have had any significant peculiar velocities removed and they have arrived at the centre of cluster through dynamical friction.

However, there is a growing body of evidence that a non-negligible fraction of clusters possess cD galaxies with significant peculiar velocities (Oegerle & Hill 2001 and references therein). Hill et al. (1988) report a cD peculiar velocity in Abell 1795 of 365 km s^{-1} . In their observations of Abell 2670, Sharples, Ellis & Gray (1988) find the cD galaxy has a peculiar velocity that is $439 \text{ km s}^{-1} - 3.7\sigma$ away from the cluster mean. Later, Bird (1994; see also Bird 1993; Oegerle & Hill 2001) showed that the cD peculiar velocity may be intimately tied to the presence of substructure in Abell 2670. Such an effect lends support to the picture of clusters growing hierarchically through repeated mergers. For the simulations of Malumuth (1992), it suggests that the formation of cD galaxies after the virialization of the cluster cannot account for such cD peculiar velocities. Therefore some or all of the following could be true: (1) clusters that form cD galaxies are necessarily young; (2) cD galaxies are a relatively recent occurrence; (3) clusters of galaxies are not virialized^{*}; (4) cD galaxies do not form in their present environs, rather they have been accreted from elsewhere; (5) real Universe dynamical friction is less efficient than simulated. In this work, we present evidence for one of the largest and most significant cD peculiar velocities found to date in Abell 3653.

The format of this work is as follows. In Section 2, we describe the selection, observations and reduction of our 2dF dataset. In Section 3, we explore the redshift structure of Abell 3653 and derive its velocity and velocity dispersion. In

Section 4, we closely examine the cD galaxy of Abell 3653 and its highly peculiar velocity. In Section 5, we probe the cluster’s morphology for any sign of substructure. We discuss our findings in Section 6 before summarizing the results in Section 7. The full spectroscopic catalogue of our observation is presented in Appendix A. Throughout this work we use a cosmological concordance model with values of $H_0 = 70 \text{ km s}^{-1} \text{ Mpc}^{-1}$, $\Omega_M = 0.3$ and $\Omega_\Lambda = 0.7$.

2 DATA AND DATA REDUCTION

It is essential to note here that the original aim of our observations was to confirm or deny the presence of a dark galaxy candidate in the region (Doyle et al. 2005). Such an object is one that is visible at radio wavelengths (i.e. HI), but has no obvious optical counterpart. The dark galaxy candidate was later eliminated by other follow-up observations (see Doyle et al. 2005 for more detail). However, the 2dF data gathered for that aim were approximately centered upon Abell 3653 and, here, we describe this unique dataset in full.

2.1 Observations

Our observations for this work come from 2dF spectroscopy and are summarized in Table 1 whilst we present our final catalogue in Appendix A. These observations are entirely performed in service mode on the AAT, meaning that we have a mixture of gratings (300B and 270R), and physical conditions. Regardless, all of our observations are approximately centred on $[\text{OIII}]\lambda 5007\text{\AA}$ which gives us coverage of major spectral lines such as $\text{H}\alpha$, $\text{H}\beta$, $\text{H}\gamma$, $\text{H}\delta$, and (for many) Ca K & H at the median redshift of Abell 3653 ($z \sim 0.1$) – i.e. more than adequate to provide plentiful features to measure redshifts with.

We note that 2dF has fibres that range in size from $2.16''$ diameter on the optical axis to $1.99''$ at the edge of a two degree field. At the adopted cluster distance, $1''$ corresponds to 1.941 kpc , giving an aperture size of $4.19\text{--}3.86 \text{ kpc}$ depending upon where a fibre is placed. We note that the cD galaxy is near the centre of the 2dF field, but nevertheless, the measured velocity for the cD may be biased if there are multiple nuclei present.

The galaxies chosen for spectroscopic observation are derived from the APM catalogue (e.g. Maddox et al. 1990; see also www.ast.cam.ac.uk/~mike/apmcat/). Our broad aim is to sample this region of the sky without bias to colour or galaxy type, down to a limiting magnitude of $R \approx 18$ (roughly corresponding to $M^* + 1.5$ at the redshift of Abell 3653) in order to probe sufficiently deep in the luminosity function (i.e. to eliminate all obvious bright galaxies that might have been optical counterparts to the dark galaxy candidate in the region; Doyle et al. 2005). Therefore we select all objects within the 60 arcmin of the nominal cluster centre ($\alpha = 19 \ 52 \ 37$, $\delta = -52 \ 01 \ 14$; NASA Extra-galactic Database[†]). Further, we made no attempt to

[†] The NASA/IPAC Extragalactic Database (NED) is operated by the Jet Propulsion Laboratory, California Institute of Technology, under contract with the National Aeronautics and Space Administration.

^{*} i.e. the mean velocity of the galaxies does not represent the cluster velocity.

Table 1. Summary of 2dF observations. Note that the majority of observations made on 28 July 2005 are re-observed in subsequent configurations. Each configuration, N(config), refers to one 2dF CCD worth of observations, equivalent to a total 200 fibres. N(obs) is the number of fibres out of the 200 possible fibres that are allocated to our spectroscopic targets; the remainder are divided between sky fibres and unused (or) dead fibres.

Observation Date	N(config)	Integration Time (s)	Grating	Seeing (arcsec)	N(obs)
28 July 2005	1	1 × 1800	300B	1.6–2.2	183
9 August 2005	2	3 × 1800	270R	1.2–1.8	134, 130
10 August 2005	1	3 × 1800	270R	1.7–1.9	160

exclude stars from our selection so that we would not bias ourselves to excluding more compact galaxies; akin to the approach adopted by Drinkwater et al. (2003) in the nearby Fornax and Virgo clusters. As noted by Drinkwater, this is an observationally expensive technique that in our case results in almost as many stars being observed as galaxies. The APM positional accuracy (Maddox et al. 1990) is better than $0.3''$ for all galaxies – sufficient for 2dF observations and is also the same approach used by Colless et al. (2001) for the Galaxy Redshift Survey.

For 2dF observing, each of our target objects is given a priority in the CONFIGURE software package (see www.aao.gov.au/2df/manual/) that is proportional to its R -band magnitude to ensure that the brighter objects (e.g. cD type galaxies) are definitely observed whilst the more common (numerous) fainter galaxies are less likely to be sampled. Sky fibres are then allocated and checked to ensure that they are blank sky and not accidentally placed upon actual objects. Figure 1 displays the fraction of objects that are observed out of all possible candidate objects. At $R < 18$, we are at least 60 per cent likely to place a fibre on a given object. This fraction drops rapidly toward fainter magnitudes.

2.2 Reduction

Our data are reduced in a standard manner in the automated 2dF data reduction pipeline software (www.aao.gov.au/2df/; see also Bailey et al. 2001).

Redshift determination is carried out using the ZCODE package, as employed by 2dFGRS (Colless et al. 2001) and 2SLAQ (Cannon et al. 2005). Briefly, our objects are cross-correlated with a number of template spectra (including G- and K-type stars; a globular cluster and several galactic spectra). Each resultant redshift is given a Tonry & Davis (1979) value (TDV) in order to determine which template spectra provides to best redshift – usually the one with the highest TDV. To check this, each spectra is de-redshifted to rest frame wavelengths and inspected by eye (KAP & IGR) to check that its emission and absorption features confirm the redshift determination. At this stage, we give a *qualitative* quality parameter to the resultant redshift in the range 1 to 4. A value of 4 denotes a certain redshift (all spectral features, both emission and absorption are in the correct place, the spectra has a good signal to noise ratio and/or TDV with an obvious single cross-correlation peak). A quality of 3 is given to a spectra that is very probably correct (it

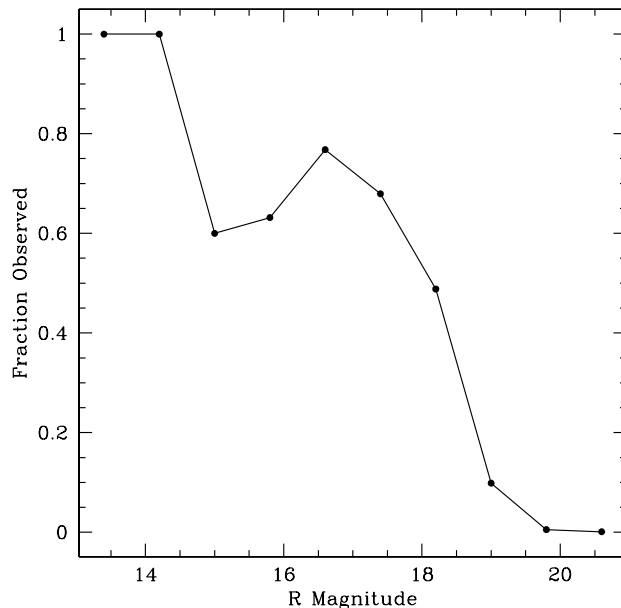


Figure 1. Fraction of galaxies from the parent APM catalogue that are selected for observation with 2dF. Since brighter objects are given a higher priority flag in the 2dF configurations, they are the most likely to have a fibre placed upon them.

has many or all of the spectral features in the right locations and a reasonable S/N ratio). A quality of 2 is given to those spectra that are only 50 per cent likely to be correct (typically only two spectral lines are present and S/N and TDV are low with perhaps two or more plausible cross-correlation peaks). A quality of 1 denotes a galaxy that we could not even guess a redshift for. We note that all redshifts used in this work are heliocentric.

The fraction of our observations that yield a quality 3 or 4 is shown in Figure 2 as a function of magnitude. At bright magnitudes ($R < 18$), the redshift completeness is always above 80 per cent. This drops markedly for fainter magnitudes. Multiplied together with Figure 1, these fractions define our overall survey function (i.e. how likely a galaxy is to be observed and how likely that observation is to produce a quality redshift). In principle, there are of course other selection and completeness limits in this survey beyond Figures 1 and 2. For example, only one galaxy in a close pair of galaxies are likely to be observed as there is a

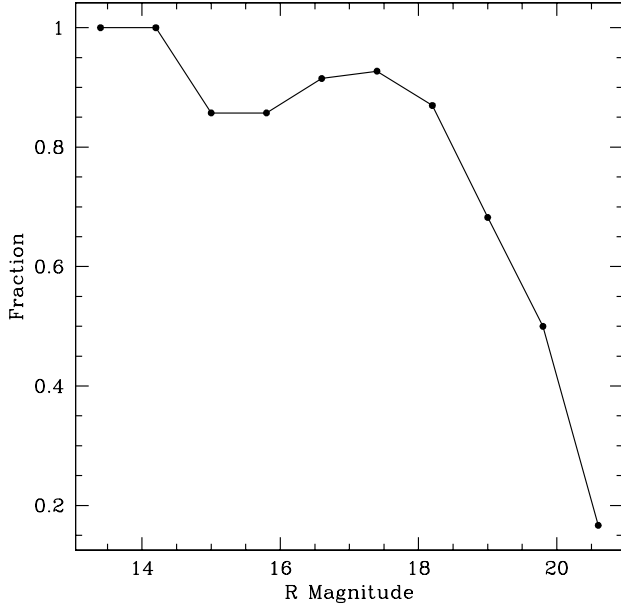


Figure 2. Spectroscopic success rate, defined as the fraction of spectra that give a quality 3 or 4 redshift, as a function of magnitude. All of the bright spectra generate a definite redshift, decreasing to fainter magnitudes.

limit to how close 2dF can place fibres next to each other without causing problems. Since we observe with multiple configurations of 2dF, we consider such geometric selection effects to be minimized and hence consider the product of Figures 1 and 2 to be a good approximation for the final overall survey function.

For the rest of this work, we will stick to only those galaxies with a quality parameter of 3 or 4 to ensure that our redshifts are of excellent quality.

2.3 Duplicate observations

Intentionally, observations of some objects are repeated from one 2dF configuration to another. This provides us with a means to evaluate our own internal error rates.

For our quality 2 objects that have a better quality repeat, we find that roughly only half of them are within 300kms^{-1} of the original measurement.

Out of the 489 objects (of quality 3 or 4) observed, 293 are unique objects with no secondary observation made. The remaining objects are multiple (usually 2 observations, occasionally 3) observations of a further 98 objects[‡].

For these 98 repeat observations, the median absolute difference in redshift measurement is $|\Delta z| = 0.00022$ (or about 66 km s^{-1}). Moreover, none of them deviate by more than 300 km s^{-1} from their duplicate. This is very comparable to the same measurement performed by 2dFGRS of 64 km s^{-1} (Colless et al. 2001) and by LARCS of 65 km s^{-1} (Pimblet et al. 2006). The very similar values are expected

[‡] Therefore, in total, we have observed 391 individual objects with a quality flag or 3 or 4. See Appendix A.

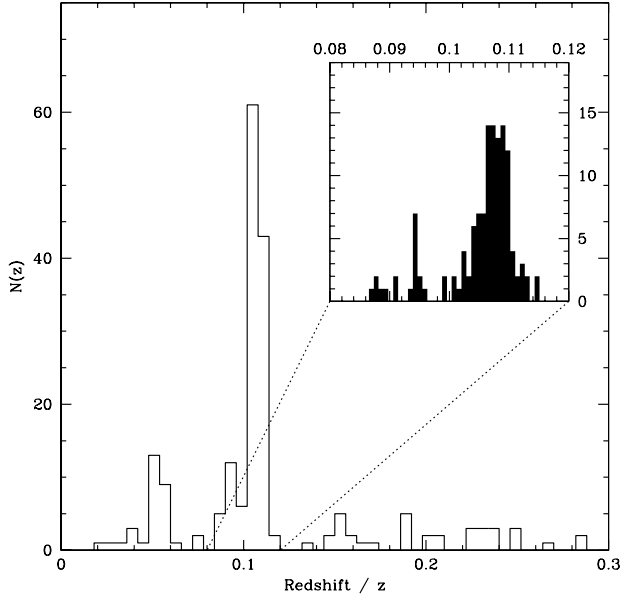


Figure 3. Redshift histogram for Abell 3653 with an inset panel depicting a magnification of the central region. Abell 3653 appears to be a reasonably regular cluster with a couple of groups in the foreground. A secondary structure can also be seen at $z \sim 0.05$. We suggest that this may be part of Abell S0835.

given the highly similar way in which these surveys all process their datasets. Significantly, we find no dependence of this value on the redshift of a given object.

For our final catalogue (Appendix A), we remove the duplicated objects. This is done by selecting the object that has the highest quality flag, then the highest TDV (in the event of a pair having the same quality) for inclusion in the final catalogue. We also note that the cD galaxy did not have any repeat observations made.

3 REDSHIFT STRUCTURE

Of the 391 objects in our final catalogue, 191 (48.8 per cent) have redshifts $z < 0.01$ and are therefore classified as stars. For the galaxies in our sample, we now construct a redshift histogram to qualitatively examine the cluster structure and to aid in defining cluster membership (Figure 3).

Figure 3 suggests that Abell 3653 is a reasonably regular cluster (approximately a Gaussian shape) with only minor sub-structure and a couple of close galaxies or groups of galaxies around it in redshift space. A secondary structure is also seen at $z \sim 0.05$. To get a better qualitative assessment of the overall appearance of these structures, we create wedge plots of redshift versus the RA and Dec of our observed galaxies (Figure 4).

The wedge plots show that the bulk of the cluster is contained at around $z \approx 0.11$, and it appears to be slightly elongated in RA compared to Dec. It is also a relatively isolated cluster: there are almost no galaxies in the immediate background, with a couple of galaxies in the foreground. In the line of sight to the cluster, we again note that there are structures at $z \approx 0.05$ and 0.06 which do not appear tightly

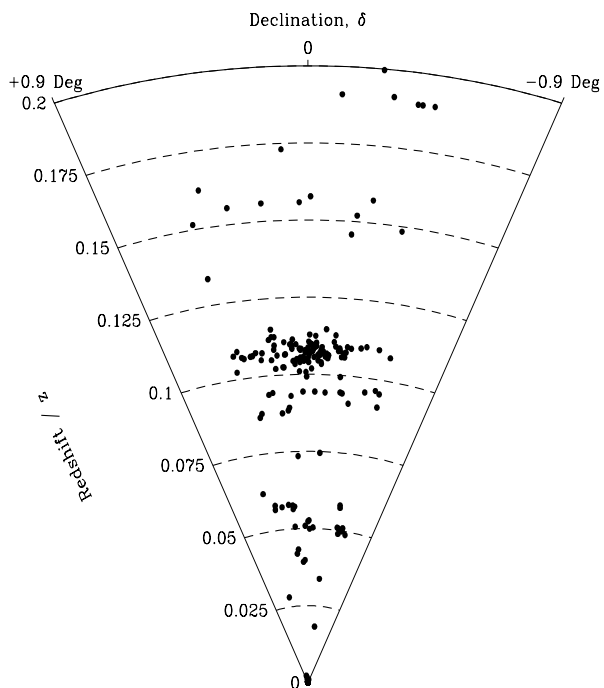
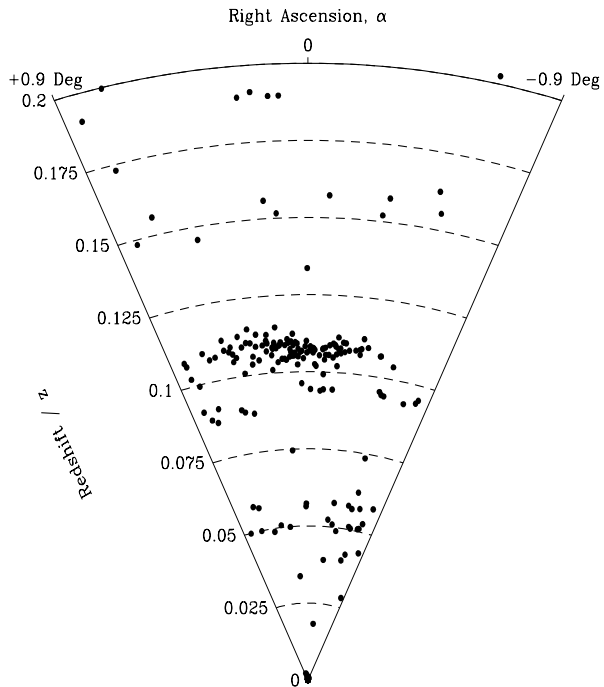


Figure 4. Wedge plots of right ascension and declination versus redshift in the direction of Abell 3653. The centre of the cluster is located at $\alpha = \delta = 0$.

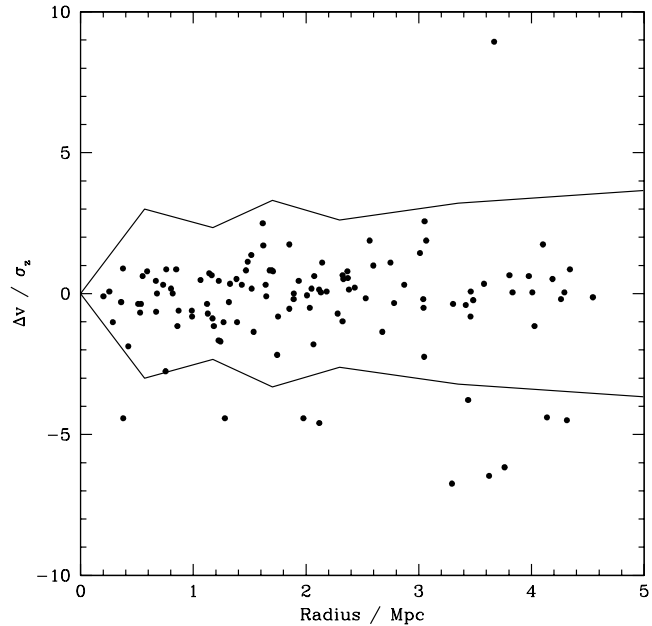


Figure 5. Phase-space diagram of Abell 3653: radius from the cluster centre is plotted as a function of velocity difference from the cluster mean. The solid lines are the 3σ rms scatter for the cluster members. All galaxies within these lines are considered cluster members.

bound and may therefore be foreground groups or perhaps the periphery of Abell S0835 (located over 1 degree away from Abell 3653 at $z \sim 0.05$).

3.1 Cluster Membership and Velocity Dispersion

To define cluster membership we employ the statistical clipping technique of Zabludoff, Huchra & Geller (1990; ZHG) to find the cluster's mean velocity, cz , and velocity dispersion, σ_z . ZHG is an iterative technique whereby the entire cluster population is looped over repeatedly. Any galaxy that is more than $1\sigma_z$ from their nearest neighbour are flagged for exclusion. This process is then repeated, excluding the flagged galaxies, until convergence of the galaxy population is achieved.

We find that ZHG gives values of $cz = 32214 \pm 83 \text{ km s}^{-1}$ and $\sigma_{cz} = 880_{-54}^{+66}$, with 111 cluster members. The errors on the velocity dispersion and mean velocity are taken using the formulae presented by Danese, De Zotti and di Tullio (1980). This redshift is in good agreement with previous estimates (e.g. 32670 km s^{-1} from Struble & Rood 1999) and confirms that the earlier estimate of Abell, Corwin & Olowin (1989) of 14250 km s^{-1} refers to the secondary structure highlighted by Figure 3 at $z \sim 0.05$.

4 CD PECULIAR VELOCITY

Using the mean velocity of Abell 3653, $cz = 32214 \pm 83 \text{ km s}^{-1}$, we now proceed to evaluate the peculiar velocity of the cluster cD galaxy. In Appendix A, the cD galaxy is recorded as entry PRD196 and has a velocity of $cz = 32970$

kms^{-1} with an assumed error of $\pm 66 \text{ kms}^{-1}$ (see above)[§]. The cD galaxy has also been previously observed by Postman & Lauer (1995) who find a velocity of $cz = 32739 \pm 97 \text{ kms}^{-1}$. The difference between our measurement and that of Postman & Lauer (1995) is less than 2σ and therefore we do not regard it as highly significant. Moreover, this reduces the likelihood that the cD galaxy possesses multiple nuclei that could contaminate our measurement due to random fibre placement.

The errors of the cD galaxy and the cluster are now added in quadrature to give a peculiar motion of the cD galaxy of $756 \pm 106 \text{ kms}^{-1}$ using our velocity for the cD galaxy. If we use the velocity of the cD galaxy found by Postman & Lauer (1995) it would be $525 \pm 128 \text{ kms}^{-1}$. These values must be corrected by a $(1+z)$ factor to obtain the peculiar velocity in the cluster rest frame. This correction gives values of $683 \pm 96 \text{ kms}^{-1}$, and $474 \pm 116 \text{ kms}^{-1}$, respectively. We note that these two peculiar velocities are well within 2σ of each other. Interestingly, they are *significantly* higher than our cluster velocity, by $4.1\text{--}7.1\sigma$. We therefore reject the assumed null hypothesis that the cD galaxy lies at the very centre of our cluster velocity distribution with a confidence level of $\gg 99.9$ per cent.

Such a cluster restframe peculiar velocity is also rather large – we believe that it may be the largest peculiar velocity ever reported in the literature. In Abell 2670, Sharples et al. (1988) report a peculiar velocity of 439 kms^{-1} – one of the largest peculiar motions previously reported in the literature for a cD galaxy. Indeed, most cD galaxies *are* found at the centre of their host cluster velocity distribution (Oegerle & Hill 2001; Quintana & Lawrie 1982). We note, however, that these studies have used cluster galaxies that have a much more confined radial extent from the cluster centre (or a different magnitude limit) than those presented in this work, generally at least within 3 Mpc. To ascertain if this has any effect on the cD peculiar velocity, we now re-compute the cluster’s velocity using the ZHG method, but restrict our sample in both radius and magnitude. The results of this analysis are presented in Table 2. Neither restricting the sample in radius from the cluster centre or magnitude makes the peculiar velocity of the cD galaxy insignificant.

5 CLUSTER MORPHOLOGY

In Figure 6 we plot the positions of cluster members smoothed with a Gaussian kernel of length 0.5 Mpc. The cluster appears to be quite regular in shape, with only a mild elongation in right ascension compared to declination. We also note that the cD galaxy is located just off the NED adopted cluster centre by about 0.7 Mpc.

To better probe the internal structure of the cluster, we now apply the Dressler & Shectman (1988; DS herein) test to search for any sign of substructure. We elect to use the DS approach as a lack of consensus concerning the optimal tool to use for the detection of substructure led Pinkney et al. (1996) to investigate differences among a battery of statistical tools. They conclude by endorsing the DS test as by

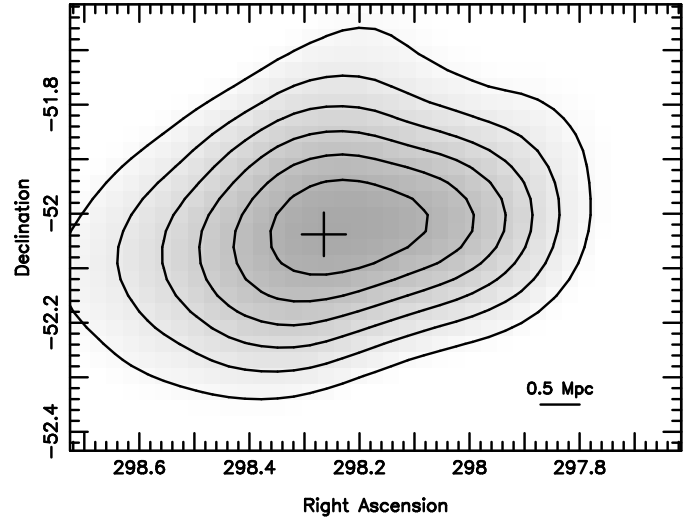


Figure 6. A smoothed spatial distribution of galaxies belonging to Abell 3653. The positions of the galaxies are smoothed with a Gaussian kernel of length 0.5 Mpc at the mean redshift of the cluster (scale bar in the lower right). The lowest contour represents a surface density of 3 Mpc^{-2} and each contour interior to this increases by 1 Mpc^{-2} . The central crosshair denotes the location of the cD galaxy. The cluster displays a mild elongation in RA compared to Dec., but is otherwise quite regular morphologically.

far the most powerful and most sensitive (three-dimensional) substructure detection tool available in the general case. The DS method is briefly outlined below.

For each cluster member, its ten nearest neighbours on the sky are found. For this group of 11 galaxies, the *local* mean velocity, \bar{v}_{local} , and velocity dispersion, σ_{local} is calculated and compared to the corresponding global values. Thus the deviation is:

$$\delta_i^2 = (11/\sigma^2)[(\bar{v}_{local} - \bar{v})^2 + (\sigma_{local} - \sigma)^2] \quad (1)$$

The parameter of merit, however, is the cumulative deviation, Δ , which is the sum of all δ_i for the N cluster members:

$$\Delta = \sum_{i=1}^N \delta_i \quad (2)$$

For a cluster velocity dispersion which is Gaussian in nature, the Δ statistic will be of order N . As the underlying distribution may not be Gaussian even for a cluster without substructure, 1000 Monte-Carlo simulation are run on the clusters, each time shuffling the galaxies velocities but holding their positions constant. Caution must be exercised as should substructure be aligned along the line of sight to the cluster, the Δ statistic will not show this.

From the DS test we obtain $N = 111$ and find that $\Delta_{Obs} = 135$, with the average simulation producing $\Delta_{Av} = 122$, and the most deviant simulation giving $\Delta_{max} = 178$. This yields $P(\Delta) = 0.169$ meaning that Abell 3653 does not have any significant substructure over the entire spatial range probed. Moreover, $P(\Delta)$ does not become significant (i.e. < 0.001) over any range of radius from the cluster centre. Our result from the DS test is illustrated in Figure 7. Each galaxy is marked with a circle whose diameter is proportional to e^δ , therefore any subclustering would be seen

[§] The position of the cD galaxy is $19\ 53\ 3.52\ -52\ 02\ 16.2$, with $TDV = 5.4$, a magnitude of $R = 11.2$ and a quality flag of 4.

Table 2. Cluster velocity measurements via ZHG for a variety of samples. The column headed ‘cD cz significance’ lists how significant our measurement of the peculiar velocity of the cD galaxy is away from the cluster velocity measurement for each given sample.

Sample Restriction	N(gal)	cz (kms^{-1})	σ_{cz} (kms^{-1})	cD cz significance
unrestricted	111	32214 ± 83	880^{+66}_{-54}	7.1σ
$r < 1.0$ Mpc	24	31986 ± 159	780^{+147}_{-94}	5.7σ
$r < 2.0$ Mpc	59	32154 ± 114	878^{+95}_{-71}	6.2σ
$r < 3.0$ Mpc	83	32207 ± 92	837^{+74}_{-58}	6.7σ
$R < 17.5$	33	32155 ± 147	844^{+129}_{-83}	5.1σ
$R < 18.0$	60	32152 ± 110	855^{+91}_{-69}	6.4σ
$R < 18.5$	90	32214 ± 87	827^{+70}_{-56}	6.9σ

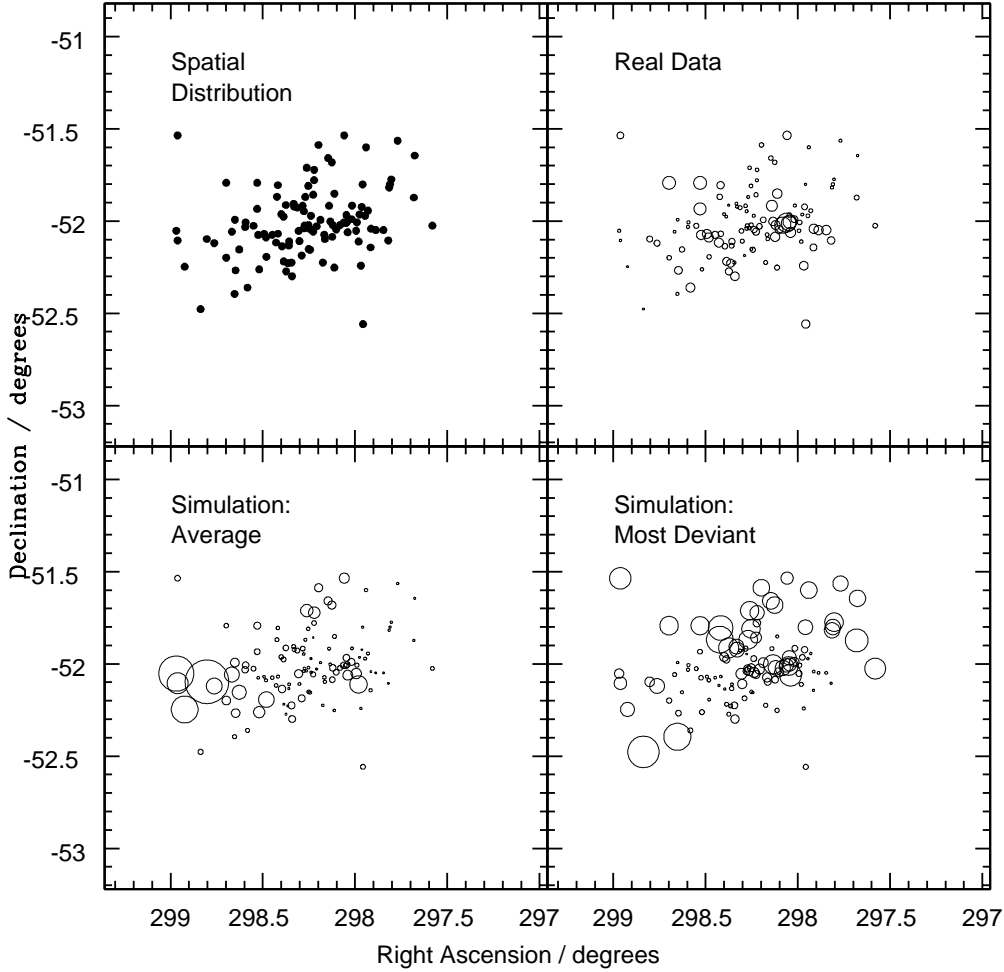


Figure 7. Spatial distribution and the results of the DS tests. Top Left: the spatial distribution of cluster members. Top Right: DS test of the actual data. Bottom Left: average of the 1000 Monte-Carlo simulations. Bottom Right: most deviant of the 1000 Monte-Carlo simulations. Abell 3653 does not exhibit any significant subclustering.

as a localized group of overlapping circles. Figure 7 confirms that there is no significant substructuring within the cluster.

6 DISCUSSION

It is certain that the presence of substructure will affect the cluster velocity and velocity dispersion – thereby perturbing the peculiar velocity measurement of the cD galaxy. Equally, during a cluster-cluster merger, the cD galaxy may be relocated from its assumed position at the bottom of the gravitational potential well of the cluster (Zabludoff & Zaritsky 1995). However, since Abell 3653 shows no sign of significant subclustering on any scales (i.e. in any radially-limited subset of the cluster members), we conclude that the peculiar velocity of the cD galaxy cannot be due to perturbations of the mean cluster velocity arising from infalling galaxy groups or subclusters.

It is possible that the cD galaxy is a part of a very localized subclump. There are 9 galaxies in close proximity (within 5 arcmin) of the cD galaxy. Using ZHG, the systemic velocity of these 9 galaxies is $32323 \pm 204 \text{ km s}^{-1}$. Thus the cluster restframe peculiar velocity of the cD galaxy to those galaxies in close proximity to it is $584 \pm 214 \text{ km s}^{-1}$. This is just under 3σ and gives a confidence level of > 99.5 per cent to reject the null hypothesis that the cD galaxy is at the centre of this local group of galaxies. Although the DS test has been endorsed as one of the best tests around for finding substructure (Pinkney et al. 1996), we can consider if it would be capable of detecting a small group around the cD galaxy. We do this by giving the 9 galaxies around the cD galaxy a velocity appropriate to a small group (say up to $\sigma_{cz}=350 \text{ km s}^{-1}$), repeating the DS test and then performing a Monte-Carlo simulation of this analysis 100 times. We find that the DS test is able to pick them up as a significant substructure within the cluster in all cases.

Within this sample, however, there are 3 galaxies that have redshifts that are very close to that of the cD galaxy. It may be the case that the cD galaxy formed very early in the evolution of a cluster (Merritt 1985). Consider a small group that collapses and subsequently virializes. Such a system may later encounter other similar systems and merge with them to form a richer cluster (Sharples et al. 1988; White & Rees 1978). Since the cD galaxy has a large peculiar velocity, it may simply be the case that it has not had sufficient time to complete the mixing process; akin to a more advanced stage of Abell 2670 (Sharples et al. 1988). Our results favour a picture of cluster growth fuelled by the hierarchical accretion of sub-clusters and galaxy groups. Conversely, they strongly argue against a picture of cD galaxies that grow in situ, post-virialization of the cluster.

7 SUMMARY

This work presents new observations of the galaxy cluster Abell 3653 using the 2dF spectrograph to amass 391 new redshift measurements. Of these, we find 111 are bone-fide cluster members, whilst about half of them are stars owing to our non-biased approach to selecting objects for observation. Our main findings are:

- Abell 3653 has a velocity of $cz = 32214 \pm 83 \text{ km s}^{-1}$ ($z = 0.10738 \pm 0.00027$), with a velocity dispersion of $\sigma_{cz} = 880^{+66}_{-54}$. Such a value of σ_{cz} is typical for massive clusters at these redshifts (cf. Pimblet et al. 2006).
- From our data, the cD galaxy of Abell 3653 has an extremely large cluster restframe peculiar velocity of $683 \pm 96 \text{ km s}^{-1}$. This is over 7σ away from the mean cluster velocity and makes the peculiar velocity of this cD galaxy one of the largest, perhaps even the largest ever recorded for a cD galaxy. The significance and magnitude of the peculiar velocity do not change significantly by restricting our sample to brighter galaxies and / or smaller radii from the cluster centre.
- Using a DS test, Abell 3653 shows no sign of significant subclustering on any length scale. Therefore the peculiar velocity of the cD galaxy cannot be accounted for by considering recent (major) cluster merger events.
- Our results favour a scenario whereby rich clusters grow in a hierarchical fashion from sub-clumps and groups infalling into a gravitational potential well. They do not favour theories which require a cD galaxy to sit at the bottom of a gravitational potential well and grow in situ there.

ACKNOWLEDGMENTS

We warmly thank the 2dF observers who carried out the observations for us in service mode at the AAT, namely Rob Sharp and Quentin Parker. We also wish to thank Michael Drinkwater for stimulating conversations that have improved this work and an anonymous referee for very useful feedback. KAP acknowledges support from an EPSA University of Queensland Research Fellowship.

REFERENCES

- Abell G. O., Corwin H. G., Olowin R. P., 1989, *ApJS*, 70, 1
 Bailey J., Taylor K., Robertson G., Barden S., 2001, *NewAR*, 45, 41
 Barnes J. E., Hernquist L., 1992, *ARA&A*, 30, 705
 Beers T. C., Geller M. J., 1983, *ApJ*, 274, 491
 Bird C. M., 1993, *PASP*, 105, 1495
 Bird C., 1994, *ApJ*, 422, 480
 Blakeslee J. P., Tonry J. L., 1992, *AJ*, 103, 1457
 Cannon R. D. et al., in prep.
 Capelato H. V., Des Forets G., Mazure A., Salvador-Sole E., 1985, *Ap&SS*, 108, 363
 Colless M. et al. 2001, *MNRAS*, 328, 1039
 Danese L., de Zotti G., di Tullio G., 1980, *A&A*, 82, 322
 Doyle M. T., et al., 2005, *MNRAS*, 361, 34
 Dressler A., Shectman S. A., 1988, *AJ*, 95, 985
 Drinkwater M. J., Gregg M. D., Hilker M., Bekki K., Couch W. J., Ferguson H. C., Jones J. B., Phillipps S., 2003, *Nature*, 423, 519
 Dubinski J., 1998, *ApJ*, 502, 141
 Duncan M. J., Farouki R. T., Shapiro S. L., 1983, *ApJ*, 271, 22
 Garijo A., Athanassoula E., Garcia-Gomez C., 1997, *A&A*, 327, 930
 Gregorini L., de Ruitter H. R., Parma P., Sadler E. M., Vettolani G., Ekers R. D., 1994, *A&AS*, 106, 1
 Hausman M. A., Ostriker J. P., 1978, *ApJ*, 224, 320
 Hill J. M., Hintzen P., Oegerle W. R., Romanishin W., Lesser M. P., Eisenhamer J. D., Batuski D. J., 1988, *ApJ*, 332, L23
 Lauer T. R., 1988, *ApJ*, 325, 49

- Maddox S. J., Efstathiou G., Sutherland W. J., Loveday J., 1990, MNRAS, 243, 692
- Malumuth E. M., 1992, ApJ, 386, 420
- Merrifield M. R., Kent S. M., 1991, AJ, 101, 783
- Merritt D., 1985, ApJ, 289, 18
- Merritt D., 1984, ApJ, 280, L5
- Nipoti C., Stiavelli M., Ciotti L., Treu T., Rosati P., 2003, MNRAS, 344, 748
- Nipoti C., Treu T., Ciotti L., Stiavelli M., 2004, MNRAS, 355, 1119
- Oegerle W. R., Hill J. M., 2001, AJ, 122, 2858
- Ostriker J. P., Tremaine S. D., 1975, ApJ, 202, L113
- Pimblet K. A., Smail I., Edge A. C., O'Hely E., Couch W. J., Zabludoff A. I., 2006, MNRAS, 366, 645
- Pinkney J., Roettiger K., Burns J. O., Bird C. M., 1996, ApJS, 104, 1
- Postman M., Lauer T. R., 1995, ApJ, 440, 28
- Quintana H., Lawrie D. G., 1982, AJ, 87, 1
- Sharples R. M., Ellis R. S., Gray P. M., 1988, MNRAS, 231, 479
- Smith R. M., Frenk C. S., Efstathiou G., Ellis R. S., Valentijn E. A., 1985, MNRAS, 216, 71P
- Struble M. F., Rood H. J., 1999, ApJS, 125, 35
- Tonry J., Davis M. 1979, AJ, 84, 1511
- Tremaine S., 1990, in Dynamics and Interactions of Galaxies, ed. R. Wielen (Berlin: Springer-Verlag), 394
- White S. D. M., Rees M. J., 1978, MNRAS, 183, 341
- Yamada T., Koyama Y., Nakata F., Kajisawa M., Tanaka I., Kodama T., Okamura S., De Propris R., 2002, ApJ, 577, L89
- Zabludoff A. I., Huchra J. P., Geller M. J., 1990, ApJS, 74, 1 (ZHG)
- Zabludoff A. I., Geller M. J., Huchra J. P., Vogeley M. S., 1993, AJ, 106, 1273
- Zabludoff A. I., Zaritsky D., 1995, ApJ, 447, L21

APPENDIX A: THE REDSHIFT CATALOGUE

Table 3 gives the final redshift catalogue for all objects observed in the direction of Abell 3653 with a quality flag of 3 or 4. Note that all redshifts are heliocentric. The full version of the spectroscopic catalogue will also be made available in Synergy, the online version of the Monthly Notices of the Royal Astronomical Society.

Table 3. The redshift catalogue. The R magnitude is sourced from the APM catalogue. Rather than providing an error on the redshift, z , which would only be the error on the cross-correlation fit, we follow 2dFGRS data release model to give the Tonry-Davis value (TDV) and our own quality assessment parameter.

Identification Tag	RA (J2000)	Dec (J2000)	R	z	TDV	Quality	Abell 3653 Member?
PRD1	19 55 15.27	-51 58 7.6	18.66	0.2279	6.04	4	
PRD2	19 55 10.84	-51 53 25.5	18.12	0.2848	9.30	4	
PRD3	19 54 7.32	-51 56 1.8	18.22	0.1034	6.22	4	yes
PRD4	19 55 12.57	-51 50 16.1	18.96	0.3220	6.91	4	
PRD5	19 55 59.11	-51 37 41.4	18.16	0.2358	5.47	3	
PRD6	19 53 15.11	-51 55 38.8	18.78	0.1044	6.37	3	yes
PRD7	19 53 30.05	-51 54 48.2	18.37	0.1098	6.26	3	yes
PRD8	19 54 12.13	-51 48 29.3	18.85	0.0003	3.76	3	
PRD9	19 54 57.22	-51 34 14.8	18.36	-0.0002	5.61	3	
PRD10	19 52 45.03	-51 59 35.6	17.20	0.1044	7.20	3	yes
PRD11	19 53 25.81	-51 48 36.1	18.39	0.1559	6.82	3	
PRD12	19 54 9.12	-51 35 26.8	18.14	-0.0004	4.54	3	
PRD13	19 54 3.77	-52 00 29.3	18.45	-0.0003	5.14	3	
PRD14	19 52 26.82	-51 51 5.0	17.36	0.1025	6.25	3	yes
PRD15	19 52 40.87	-51 54 14.0	18.80	0.0004	9.01	4	
PRD16	19 52 18.02	-51 30 41.5	17.93	0.0001	4.78	3	
PRD17	19 52 14.75	-51 39 51.0	18.28	0.0001	4.39	4	
PRD18	19 52 32.37	-52 00 8.1	18.14	0.1071	6.90	3	yes
PRD19	19 50 55.29	-51 41 12.6	18.10	0.0001	5.43	3	
PRD20	19 51 8.84	-51 32 42.7	17.65	0.0002	12.80	4	
PRD21	19 51 16.34	-51 29 49.4	17.90	-0.0003	3.97	3	
PRD22	19 50 9.19	-51 33 57.8	17.22	0.0002	5.93	3	
PRD23	19 51 12.93	-51 46 26.7	18.53	0.1116	3.03	3	yes
PRD24	19 51 14.49	-51 48 1.2	18.67	0.1083	7.18	3	yes
PRD25	19 49 44.42	-51 53 40.4	17.48	0.0931	3.30	4	
PRD26	19 51 43.20	-51 56 37.5	17.61	0.1098	6.79	3	yes
PRD27	19 49 31.34	-51 40 59.2	18.37	0.0000	5.13	3	
PRD28	19 50 10.10	-51 45 49.7	18.14	0.0001	4.12	3	
PRD29	19 52 10.47	-52 00 14.8	17.94	0.1079	7.78	3	yes
PRD30	19 49 39.52	-52 02 32.2	18.49	0.0003	13.70	4	
PRD31	19 51 23.09	-52 02 54.6	17.92	0.1076	7.05	3	yes
PRD32	19 50 27.53	-52 15 27.8	17.38	0.0945	5.24	3	
PRD33	19 50 49.45	-52 09 5.6	18.45	0.2504	7.60	4	
PRD34	19 49 34.02	-52 23 21.7	16.84	-0.0002	5.24	3	
PRD35	19 52 24.52	-52 02 43.7	18.78	0.1019	6.80	3	yes
PRD36	19 50 15.31	-52 23 17.0	18.19	0.0000	5.21	3	
PRD37	19 50 23.25	-52 29 51.1	17.72	0.0509	3.31	3	
PRD38	19 50 35.29	-52 29 0.2	18.28	0.0000	4.41	4	
PRD39	19 50 53.30	-52 25 35.8	18.31	0.0002	4.99	3	
PRD40	19 50 59.64	-52 26 17.7	18.25	-0.0002	5.94	3	
PRD41	19 51 45.13	-52 25 38.4	18.40	0.0002	8.02	4	
PRD42	19 51 6.75	-52 25 12.7	19.17	0.2048	6.23	3	
PRD43	19 51 35.87	-52 32 4.5	18.70	0.2314	7.43	4	
PRD44	19 51 55.55	-52 06 40.8	18.04	0.1089	5.80	3	yes
PRD45	19 52 40.95	-52 24 12.5	17.60	0.0000	6.53	3	
PRD46	19 52 48.57	-52 30 38.0	18.78	0.0963	3.83	3	
PRD47	19 52 50.02	-52 27 26.5	18.10	0.0002	5.55	3	
PRD48	19 52 39.28	-52 05 49.2	17.70	0.1063	4.29	4	yes
PRD49	19 52 58.66	-52 09 19.7	18.32	0.1063	6.78	3	yes
PRD50	19 52 40.06	-52 04 24.7	18.23	0.1100	6.80	3	yes
PRD51	19 53 21.90	-52 17 56.3	17.83	0.1089	7.16	3	yes
PRD52	19 54 36.77	-52 23 41.2	18.05	0.1099	4.00	3	yes
PRD53	19 54 51.28	-52 22 3.9	17.55	0.0001	5.68	3	
PRD54	19 53 12.18	-52 07 55.2	16.02	0.0746	4.79	3	
PRD55	19 55 20.96	-52 28 37.2	17.07	0.1095	6.76	3	yes
PRD56	19 55 6.36	-52 30 29.5	17.52	0.0003	6.26	3	
PRD57	19 53 25.84	-52 06 38.8	17.90	0.1034	6.34	3	yes
PRD58	19 54 18.48	-52 11 35.6	18.11	0.2066	4.80	3	
PRD59	19 55 51.10	-52 19 40.7	17.72	0.0911	3.43	3	
PRD60	19 54 16.35	-52 10 38.2	18.49	0.0001	24.50	4	

Table 3. continued.

Identification Tag	RA (J2000)	Dec (J2000)	R	z	TDV	Quality	Abell 3653 Member?
PRD61	19 53 4.00	-52 04 23.3	17.59	0.0001	4.69	3	
PRD62	19 55 41.49	-52 09 31.5	18.65	0.0001	4.78	3	
PRD63	19 55 57.85	-52 09 45.7	18.94	0.2862	5.23	4	
PRD64	19 55 12.77	-52 05 50.0	17.93	0.1070	6.40	3	yes
PRD65	19 55 58.62	-52 08 45.7	18.30	0.1910	8.39	3	
PRD66	19 54 5.99	-52 04 31.2	17.78	0.1103	7.78	3	yes
PRD67	19 55 50.86	-52 06 18.5	19.48	0.1065	3.48	3	yes
PRD68	19 54 7.45	-52 00 23.5	17.16	0.0001	5.38	4	
PRD69	19 55 45.79	-51 54 43.2	18.43	0.1731	4.31	3	
PRD70	19 54 42.29	-51 52 37.4	18.05	0.0893	6.59	3	
PRD71	19 55 60.00	-51 43 54.8	18.21	-0.0003	4.48	3	
PRD72	19 54 47.58	-51 47 33.7	20.56	0.1125	2.76	3	yes
PRD73	19 55 36.62	-51 42 2.2	18.34	0.0002	5.96	4	
PRD74	19 56 2.33	-51 38 28.9	18.09	0.0000	10.81	4	
PRD75	19 54 26.77	-51 45 46.6	18.14	0.0002	9.85	4	
PRD76	19 55 40.02	-51 31 47.7	17.38	0.0001	14.54	4	
PRD77	19 53 19.94	-51 54 21.1	17.09	0.1098	7.51	3	yes
PRD78	19 53 8.08	-51 55 2.3	18.01	0.1095	7.54	3	yes
PRD79	19 53 41.68	-51 52 6.9	18.22	0.1106	4.89	4	yes
PRD80	19 53 40.52	-51 48 19.3	17.41	0.1097	7.26	3	yes
PRD81	19 54 41.11	-51 35 7.4	17.56	0.0000	4.39	4	
PRD82	19 52 53.13	-51 43 20.2	18.09	0.1075	7.52	3	yes
PRD83	19 52 47.47	-51 35 14.9	18.07	0.1068	7.75	3	yes
PRD84	19 52 42.56	-51 42 21.6	16.95	0.0573	5.02	4	
PRD85	19 52 16.52	-51 57 17.7	18.28	0.0000	7.31	3	
PRD86	19 52 10.63	-51 45 40.4	17.53	0.0944	4.21	4	
PRD87	19 51 45.78	-51 36 1.0	18.01	0.1063	2.85	4	yes
PRD88	19 51 37.69	-51 36 57.7	18.99	0.2322	8.03	4	
PRD89	19 51 28.41	-51 46 21.9	18.59	0.0000	4.09	3	
PRD90	19 52 4.00	-51 54 57.0	17.49	0.1087	7.40	3	yes
PRD91	19 50 22.37	-51 41 30.3	18.02	0.0008	5.03	3	
PRD92	19 50 13.20	-51 39 22.1	18.30	0.1554	7.27	3	
PRD93	19 51 51.32	-51 55 22.6	18.15	0.1114	7.21	4	yes
PRD94	19 49 20.70	-51 38 18.7	18.30	0.0004	4.46	4	
PRD95	19 50 39.07	-51 50 9.9	18.25	0.0576	3.82	4	
PRD96	19 50 8.81	-51 50 46.1	18.14	0.0419	3.52	4	
PRD97	19 50 4.47	-51 54 13.9	18.24	0.0000	5.34	4	
PRD98	19 51 54.69	-51 59 1.5	18.26	0.0944	6.65	3	
PRD99	19 50 18.56	-51 58 12.7	19.32	0.0398	3.70	4	
PRD100	19 49 37.91	-51 57 52.5	17.40	0.0003	4.55	4	
PRD101	19 52 29.00	-52 01 17.0	17.77	0.1076	7.02	3	yes
PRD102	19 51 34.14	-52 01 20.4	18.07	0.0523	3.64	3	
PRD103	19 50 8.13	-52 08 48.5	18.29	-0.0003	4.59	3	
PRD104	19 51 26.98	-52 04 47.6	17.84	-0.0001	14.56	4	
PRD105	19 50 16.76	-52 05 22.8	16.45	0.0504	5.03	4	
PRD106	19 49 33.98	-52 05 51.4	18.47	0.0000	11.86	4	
PRD107	19 49 14.51	-52 06 14.0	18.23	0.0001	4.89	3	
PRD108	19 49 57.38	-52 13 38.1	18.18	0.2026	4.41	3	
PRD109	19 49 20.37	-52 18 35.4	17.93	0.0002	5.42	3	
PRD110	19 51 49.02	-52 03 59.9	18.40	0.0000	4.61	4	
PRD111	19 50 22.49	-52 16 21.7	18.13	0.0942	5.57	4	
PRD112	19 50 53.09	-52 14 18.0	18.17	0.0003	4.13	3	
PRD113	19 51 15.39	-52 14 46.5	18.42	0.1520	7.67	3	
PRD114	19 50 11.94	-52 26 46.1	18.23	0.0002	4.92	4	
PRD115	19 50 57.12	-52 19 28.6	18.41	-0.0001	4.47	4	
PRD116	19 51 16.92	-52 16 9.2	17.38	0.2497	11.96	4	
PRD117	19 51 50.94	-52 16 13.2	19.38	0.0183	5.19	4	
PRD118	19 51 21.16	-52 29 37.9	18.23	0.0003	4.28	3	
PRD119	19 51 40.41	-52 14 11.0	18.11	-0.0002	4.92	3	
PRD120	19 52 27.11	-52 15 7.3	17.94	0.1071	7.88	3	yes
PRD121	19 52 41.98	-52 13 28.2	18.89	0.1083	6.45	3	yes
PRD122	19 53 13.25	-52 26 38.9	19.01	0.1897	5.17	3	
PRD123	19 53 15.76	-52 15 22.0	18.06	0.0338	3.14	4	

Table 3. continued.

Identification Tag	RA (J2000)	Dec (J2000)	R	z	TDV	Quality	Abell 3653 Member?
PRD124	19 53 32.76	-52 13 6.8	18.56	0.1078	6.29	3	yes
PRD125	19 55 50.32	-52 29 13.9	18.79	0.2646	6.72	3	
PRD126	19 56 0.70	-52 29 14.3	17.72	0.0003	5.40	3	
PRD127	19 53 55.42	-52 11 37.1	16.98	0.1129	5.31	4	yes
PRD128	19 55 52.87	-52 27 49.8	18.26	0.1484	5.52	3	
PRD129	19 55 26.34	-52 21 35.6	18.14	0.0003	13.43	4	
PRD130	19 53 35.00	-52 08 10.1	17.15	0.1058	7.47	3	yes
PRD131	19 55 45.95	-52 13 0.1	18.14	-0.0005	5.01	3	
PRD132	19 53 13.44	-52 03 12.4	18.27	0.1088	3.17	4	yes
PRD133	19 53 5.80	-52 01 30.0	18.41	0.1074	7.65	3	yes
PRD134	19 55 39.81	-52 05 27.1	18.44	-0.0001	5.56	3	
PRD135	19 54 40.34	-52 03 28.4	18.04	0.1084	6.27	3	yes
PRD136	19 53 52.80	-52 02 14.4	18.24	0.0003	13.47	4	
PRD137	19 54 45.19	-52 02 2.7	18.20	0.0002	5.62	3	
PRD138	19 54 12.17	-52 01 33.0	17.66	0.1106	5.89	3	yes
PRD139	19 54 54.94	-52 02 6.7	17.19	0.0000	6.05	3	
PRD140	19 54 23.05	-52 01 53.9	18.15	0.1129	4.36	3	yes
PRD141	19 54 36.38	-51 59 34.4	18.24	0.1050	5.01	3	yes
PRD142	19 54 41.86	-51 43 38.3	18.68	0.2388	4.13	3	
PRD143	19 54 36.62	-51 51 59.1	19.85	0.0884	3.35	4	
PRD144	19 53 19.20	-51 55 20.5	16.42	0.1044	6.24	3	yes
PRD145	19 55 40.98	-51 36 15.1	17.52	0.0002	4.57	3	
PRD146	19 55 55.23	-51 32 40.4	16.36	-0.0002	5.34	3	
PRD147	19 55 51.01	-51 32 9.4	19.31	0.1023	3.00	4	yes
PRD148	19 53 18.89	-51 51 27.5	13.69	0.0000	5.98	3	
PRD149	19 54 26.86	-51 34 57.9	18.45	0.2335	5.00	3	
PRD150	19 54 36.58	-51 29 40.0	17.88	0.0000	5.73	3	
PRD151	19 53 6.73	-51 56 48.4	17.12	0.1050	5.08	4	yes
PRD152	19 53 34.75	-51 39 49.9	17.63	0.0003	5.82	3	
PRD153	19 52 53.34	-51 46 42.8	19.42	0.1050	3.73	4	yes
PRD154	19 52 30.20	-51 40 52.7	19.74	0.1078	4.11	4	yes
PRD155	19 52 18.71	-51 29 23.8	17.79	-0.0003	4.14	3	
PRD156	19 52 7.18	-51 33 11.4	18.70	-0.0007	4.09	3	
PRD157	19 51 0.35	-51 30 26.4	13.76	0.0001	4.31	3	
PRD158	19 50 21.23	-51 30 59.0	18.84	0.0623	3.22	3	
PRD159	19 51 24.06	-51 30 30.0	17.38	0.0002	4.40	4	
PRD160	19 50 20.41	-51 32 53.4	18.53	0.1623	6.35	3	
PRD161	19 50 37.27	-51 38 4.0	18.86	0.2371	3.47	4	
PRD162	19 49 49.16	-51 29 20.5	16.11	0.0004	8.56	4	
PRD163	19 49 47.32	-51 30 33.4	16.31	0.0002	5.11	4	
PRD164	19 51 47.99	-51 37 3.1	19.12	0.2279	3.14	4	
PRD165	19 50 25.06	-51 41 6.2	13.99	-0.0004	4.28	3	
PRD166	19 50 2.20	-51 36 5.2	16.46	0.0002	5.53	4	
PRD167	19 50 30.41	-51 50 31.9	17.26	0.0002	4.87	3	
PRD168	19 49 56.99	-51 44 55.8	17.99	-0.0004	4.62	3	
PRD169	19 50 58.36	-52 01 31.3	18.86	0.3263	3.38	4	
PRD170	19 49 21.80	-51 53 39.0	18.40	0.0002	7.31	4	
PRD171	19 49 20.35	-51 52 8.2	10.51	0.0433	4.95	3	
PRD172	19 52 4.71	-51 59 22.0	18.04	0.1056	5.69	3	yes
PRD173	19 52 13.94	-52 03 2.8	16.48	0.0000	4.74	3	
PRD174	19 49 42.22	-52 02 2.0	18.78	0.0527	2.94	4	
PRD175	19 49 8.45	-52 03 48.5	17.10	0.0003	12.75	4	
PRD176	19 49 35.06	-52 13 36.9	18.30	0.0002	4.33	3	
PRD177	19 52 11.96	-52 00 41.3	17.69	0.0993	3.60	4	yes
PRD178	19 49 36.04	-52 10 24.0	18.76	0.0008	8.29	4	
PRD179	19 49 27.10	-52 24 25.4	17.09	0.0581	3.59	4	
PRD180	19 49 48.77	-52 25 15.3	19.14	0.0509	3.25	4	
PRD181	19 51 52.34	-52 14 30.0	18.60	0.1059	6.05	3	yes
PRD182	19 52 14.69	-52 18 37.4	19.25	0.1573	2.95	4	
PRD183	19 52 9.11	-52 26 38.1	17.28	0.0004	3.91	3	
PRD184	19 51 19.93	-52 11 17.9	18.20	0.0008	3.64	3	
PRD185	19 53 28.70	-52 20 7.1	18.79	0.1913	3.33	4	
PRD186	19 53 27.48	-52 13 41.3	18.26	0.1079	5.83	3	yes

Table 3. continued.

Identification Tag	RA (J2000)	Dec (J2000)	R	z	TDV	Quality	Abell 3653 Member?
PRD187	19 54 4.78	-52 15 41.5	18.90	0.1059	4.65	3	yes
PRD188	19 54 31.16	-52 33 6.5	19.06	0.0489	3.64	4	
PRD189	19 55 23.48	-52 33 3.4	19.07	0.0911	4.17	3	
PRD190	19 55 23.18	-52 27 57.1	16.39	0.0001	13.85	4	
PRD191	19 55 13.49	-52 28 34.3	14.46	0.0499	3.02	4	
PRD192	19 53 26.21	-52 08 0.3	19.13	0.1147	4.03	4	yes
PRD193	19 55 39.76	-52 19 12.8	17.43	0.0003	4.91	3	
PRD194	19 54 35.14	-52 11 37.9	19.07	0.0002	4.41	3	
PRD195	19 55 55.08	-52 09 16.3	18.59	-0.0001	7.41	4	
PRD196	19 53 3.52	-52 02 16.2	11.21	0.1099	5.39	4	yes
PRD197	19 55 3.24	-52 07 11.8	18.86	0.1075	4.13	4	yes
PRD198	19 53 0.46	-52 09 5.1	18.85	0.1053	3.71	4	yes
PRD199	19 53 19.98	-52 10 47.6	18.92	-0.0001	5.24	3	
PRD200	19 55 50.30	-51 55 2.4	15.38	0.0001	10.36	4	
PRD201	19 55 37.48	-51 54 36.5	15.98	0.0000	10.78	4	
PRD202	19 52 46.70	-52 00 58.0	17.91	0.0000	8.30	4	
PRD203	19 53 31.84	-51 54 6.3	17.28	-0.0003	11.53	4	
PRD204	19 56 1.91	-51 44 24.4	17.82	-0.0001	7.70	4	
PRD205	19 55 36.43	-51 42 18.0	17.62	-0.0003	8.45	4	
PRD206	19 54 28.55	-51 48 26.9	17.98	0.0003	5.12	3	
PRD207	19 55 38.83	-51 43 53.0	18.38	0.0003	5.16	3	
PRD208	19 55 34.74	-51 40 4.6	18.17	-0.0004	6.16	3	
PRD209	19 55 46.20	-51 40 23.5	16.94	0.0000	6.85	3	
PRD210	19 55 45.48	-51 31 25.0	18.48	-0.0004	4.12	3	
PRD211	19 55 35.36	-51 31 7.6	17.88	0.0005	6.79	3	
PRD212	19 54 54.52	-51 43 21.1	18.60	0.0003	3.60	3	
PRD213	19 54 18.45	-51 43 32.8	18.46	0.0009	3.08	3	
PRD214	19 54 36.23	-51 42 3.3	18.67	0.0018	3.81	3	
PRD215	19 55 15.00	-51 31 21.2	17.84	0.0023	4.29	3	
PRD216	19 54 13.98	-51 30 29.0	18.45	-0.0001	5.21	3	
PRD217	19 53 46.29	-51 37 32.6	16.75	-0.0002	10.58	4	
PRD218	19 54 22.55	-51 35 33.6	18.56	0.0004	3.83	3	
PRD219	19 53 48.89	-51 52 3.3	15.34	-0.0001	14.10	4	
PRD220	19 52 54.86	-51 53 13.2	18.16	0.0001	14.94	4	
PRD221	19 54 20.27	-51 41 23.3	17.71	-0.0004	4.56	3	
PRD222	19 53 12.77	-51 29 17.0	18.65	0.1516	4.78	3	
PRD223	19 53 7.98	-51 31 27.6	17.83	0.0000	6.49	3	
PRD224	19 52 58.84	-51 44 38.5	18.49	-0.0004	5.64	3	
PRD225	19 52 52.38	-51 42 40.5	18.14	0.0003	5.73	3	
PRD226	19 52 49.82	-51 38 16.7	18.44	0.0011	4.53	4	
PRD227	19 52 44.01	-51 41 59.3	14.37	0.0002	11.44	3	
PRD228	19 52 0.38	-51 52 5.8	17.74	-0.0004	8.64	3	
PRD229	19 51 37.01	-51 43 3.6	18.85	0.0003	6.54	3	
PRD230	19 52 14.67	-52 00 29.1	17.86	0.1074	7.62	3	yes
PRD231	19 52 23.85	-52 00 32.3	18.09	-0.0005	4.06	3	
PRD232	19 51 58.20	-51 36 53.8	15.85	-0.0001	14.32	3	
PRD233	19 52 9.20	-51 46 1.1	16.67	0.0005	4.77	3	
PRD234	19 51 53.13	-51 49 40.6	18.48	-0.0001	9.69	3	
PRD235	19 50 42.36	-51 32 52.2	16.95	-0.0003	9.63	4	
PRD236	19 50 16.06	-51 29 43.8	16.83	-0.0002	7.41	4	
PRD237	19 51 9.95	-51 44 25.5	16.95	0.0001	5.72	3	
PRD238	19 49 25.53	-51 35 33.9	18.32	0.0000	5.25	3	
PRD239	19 51 22.96	-51 54 54.8	16.71	-0.0003	11.31	4	
PRD240	19 50 43.09	-51 51 7.0	18.03	-0.0002	7.56	4	
PRD241	19 51 31.23	-51 53 38.5	17.73	0.0000	11.10	4	
PRD242	19 49 59.36	-51 43 1.7	17.82	0.0003	9.99	4	
PRD243	19 50 6.28	-51 40 12.1	17.91	0.0000	4.35	3	
PRD244	19 49 19.09	-51 44 13.8	18.27	-0.0004	3.39	3	
PRD245	19 52 19.61	-52 01 18.9	17.65	0.1054	5.34	3	yes
PRD246	19 49 9.94	-51 59 17.5	17.68	0.0000	5.23	3	
PRD247	19 50 47.63	-52 12 28.9	17.29	0.0003	5.83	3	
PRD248	19 50 57.12	-52 13 2.9	18.20	-0.0002	6.63	3	
PRD249	19 50 32.31	-52 05 11.9	15.98	-0.0002	13.21	4	

Table 3. continued.

Identification Tag	RA (J2000)	Dec (J2000)	R	z	TDV	Quality	Abell 3653 Member?
PRD250	19 51 30.41	-52 11 1.8	15.09	0.0001	17.37	4	
PRD251	19 50 12.91	-52 07 9.6	17.06	0.0001	5.66	3	
PRD252	19 49 53.77	-52 10 11.8	18.19	-0.0005	4.18	3	
PRD253	19 49 36.68	-52 15 31.3	16.28	0.0001	16.95	4	
PRD254	19 49 13.63	-52 18 18.4	17.28	0.0001	7.26	4	
PRD255	19 49 29.20	-52 18 56.4	18.47	0.0000	6.18	3	
PRD256	19 49 18.89	-52 21 0.8	17.72	0.0000	5.65	3	
PRD257	19 50 22.82	-52 18 2.4	18.09	-0.0003	5.57	3	
PRD258	19 49 30.12	-52 24 33.0	16.25	0.0001	20.81	4	
PRD259	19 51 4.87	-52 15 40.2	17.97	0.0005	5.79	3	
PRD260	19 49 22.48	-52 31 48.9	15.83	-0.0001	9.57	3	
PRD261	19 49 48.67	-52 30 3.1	18.69	-0.0008	5.09	3	
PRD262	19 51 41.58	-52 14 29.5	16.07	0.0000	11.79	4	
PRD263	19 50 12.21	-52 26 25.5	18.20	-0.0001	5.80	3	
PRD264	19 50 34.38	-52 22 40.3	16.25	-0.0002	14.37	4	
PRD265	19 51 0.59	-52 30 11.0	17.52	-0.0001	8.91	4	
PRD266	19 52 12.60	-52 04 7.3	16.08	-0.0003	10.70	4	
PRD267	19 51 21.74	-52 30 39.1	15.84	-0.0001	8.74	4	
PRD268	19 52 13.58	-52 24 24.4	17.76	0.0000	4.47	3	
PRD269	19 52 9.08	-52 32 20.6	14.89	0.0011	4.76	3	
PRD270	19 51 53.23	-52 19 18.8	18.34	-0.0002	3.79	3	
PRD271	19 52 34.26	-52 07 31.1	17.12	-0.0001	6.75	3	
PRD272	19 52 22.27	-52 28 48.3	15.03	0.0001	12.46	4	
PRD273	19 53 15.21	-52 31 29.6	18.20	0.0000	10.58	4	
PRD274	19 53 7.61	-52 21 56.6	15.88	-0.0001	14.15	4	
PRD275	19 53 22.47	-52 27 19.2	12.16	-0.0001	11.67	4	
PRD276	19 53 35.45	-52 32 33.4	18.81	0.0001	24.29	4	
PRD277	19 53 4.62	-52 25 19.2	16.55	-0.0001	13.98	4	
PRD278	19 53 13.00	-52 17 45.4	16.46	-0.0003	11.42	4	
PRD279	19 53 58.33	-52 04 10.8	18.27	0.1090	3.76	3	yes
PRD280	19 53 6.55	-52 07 51.4	18.76	0.0002	3.80	3	
PRD281	19 54 40.88	-52 19 58.0	18.24	0.0004	5.31	3	
PRD282	19 53 47.75	-52 04 28.7	18.04	0.1092	5.32	3	yes
PRD283	19 53 58.70	-52 18 16.9	18.25	0.0003	4.46	3	
PRD284	19 54 51.14	-52 23 10.4	18.66	-0.0006	3.24	3	
PRD285	19 53 6.55	-52 02 20.6	18.14	0.1099	5.44	3	yes
PRD286	19 55 41.81	-52 28 34.0	17.86	-0.0001	8.47	3	
PRD287	19 55 41.77	-52 26 8.5	18.73	-0.0007	4.31	3	
PRD288	19 55 42.43	-52 21 39.4	16.91	-0.0001	11.41	4	
PRD289	19 53 42.04	-52 10 5.3	16.39	-0.0003	16.20	4	
PRD290	19 56 6.09	-52 16 29.5	17.60	-0.0001	3.43	3	
PRD291	19 56 6.30	-52 04 36.5	17.13	-0.0005	10.55	4	
PRD292	19 55 30.82	-52 03 16.0	18.74	0.0000	3.76	3	
PRD293	19 55 28.03	-52 01 6.1	17.49	0.0007	6.89	4	
PRD294	19 49 16.64	-51 40 57.8	17.98	-0.0003	5.38	3	
PRD295	19 49 18.31	-51 33 28.9	18.30	0.0281	4.41	4	
PRD296	19 49 21.12	-52 26 12.2	18.74	0.0953	3.23	3	
PRD297	19 49 24.05	-52 08 50.1	17.44	0.0942	8.63	4	
PRD298	19 49 24.70	-52 32 40.8	18.29	0.3061	4.32	3	
PRD299	19 49 25.32	-52 21 48.4	16.60	-0.0001	5.94	4	
PRD300	19 49 28.80	-51 50 21.8	18.82	0.0000	4.46	3	
PRD301	19 49 53.20	-52 26 7.6	18.36	0.0507	3.01	4	
PRD302	19 49 55.86	-52 05 47.4	17.18	-0.0001	6.82	3	
PRD303	19 50 11.59	-51 48 23.4	17.87	0.0004	6.89	4	
PRD304	19 50 19.45	-52 01 30.0	17.44	0.1040	6.05	3	yes
PRD305	19 50 21.46	-51 41 40.6	15.84	-0.0002	5.13	3	
PRD306	19 50 27.10	-51 55 39.1	17.02	0.0735	6.64	3	
PRD307	19 50 27.50	-51 37 10.0	16.35	0.0567	5.67	4	
PRD308	19 50 31.74	-52 32 36.5	18.11	0.0954	5.11	3	
PRD309	19 50 42.45	-51 38 41.9	15.93	0.1068	7.31	4	yes
PRD310	19 50 43.52	-51 52 21.3	17.72	0.1067	7.18	4	yes
PRD311	19 50 4.70	-51 51 31.2	17.39	0.0572	4.70	4	
PRD312	19 50 5.12	-51 37 48.4	18.79	0.2494	3.37	4	

Table 3. continued.

Identification Tag	RA (J2000)	Dec (J2000)	R	z	TDV	Quality	Abell 3653 Member?
PRD313	19 51 10.23	-52 01 55.3	17.69	0.1577	7.70	4	
PRD314	19 51 13.61	-52 20 25.9	16.40	0.0003	9.70	4	
PRD315	19 51 15.59	-51 49 3.9	17.49	0.1064	9.71	4	yes
PRD316	19 51 16.72	-52 06 18.5	18.72	0.1080	3.47	4	yes
PRD317	19 51 18.34	-51 58 58.6	18.86	0.0509	3.01	3	
PRD318	19 51 20.86	-52 19 41.2	17.79	0.0000	5.54	3	
PRD319	19 51 21.85	-51 47 13.3	17.33	0.0579	4.94	4	
PRD320	19 51 2.67	-52 26 49.3	18.99	0.0489	4.26	4	
PRD321	19 51 30.99	-52 26 47.5	16.67	-0.0001	10.61	4	
PRD322	19 51 32.39	-51 56 32.6	14.92	0.0392	3.51	4	
PRD323	19 51 33.12	-52 02 55.5	16.93	0.1074	8.69	4	yes
PRD324	19 51 39.34	-52 02 31.0	17.22	0.1097	3.71	4	yes
PRD325	19 51 39.83	-52 08 33.9	18.45	0.1068	6.24	3	yes
PRD326	19 51 41.80	-52 26 58.2	18.43	0.0007	5.39	4	
PRD327	19 51 4.57	-51 33 51.6	19.17	0.1089	5.31	3	yes
PRD328	19 51 46.97	-51 58 18.0	18.43	0.1079	6.81	4	yes
PRD329	19 51 49.76	-52 33 29.2	18.13	0.1075	3.80	3	yes
PRD330	19 51 50.19	-51 48 4.3	17.47	0.1021	7.95	4	yes
PRD331	19 51 54.26	-51 57 52.0	17.76	0.1084	7.06	4	yes
PRD332	19 51 57.69	-52 00 25.9	18.32	0.1048	6.62	3	yes
PRD333	19 51 58.55	-52 03 8.4	16.21	0.1093	5.90	4	yes
PRD334	19 52 11.21	-51 58 1.5	17.98	0.1040	4.68	3	yes
PRD335	19 52 12.80	-52 07 14.8	16.76	0.0000	7.16	3	
PRD336	19 52 14.09	-51 32 6.8	17.51	0.1076	7.15	4	yes
PRD337	19 52 16.36	-51 43 51.6	18.39	0.0939	3.87	4	
PRD338	19 52 29.65	-52 05 7.4	17.71	0.1063	7.85	3	yes
PRD339	19 52 33.23	-52 04 16.7	18.39	0.0944	3.91	3	
PRD340	19 52 33.84	-51 55 1.9	18.17	0.1083	7.79	3	yes
PRD341	19 52 35.11	-51 39 31.6	17.76	0.1069	7.55	3	yes
PRD342	19 52 38.59	-51 29 43.9	18.97	0.1336	3.04	4	
PRD343	19 52 43.30	-51 50 20.8	18.58	0.0564	3.48	4	
PRD344	19 52 44.32	-52 16 10.4	17.73	0.0002	4.13	3	
PRD345	19 52 49.98	-52 01 41.2	17.53	0.1065	3.16	3	yes
PRD346	19 52 54.44	-51 51 25.6	18.53	0.1024	3.09	4	yes
PRD347	19 52 54.45	-52 03 26.4	17.46	0.1092	6.93	3	yes
PRD348	19 52 57.09	-52 02 45.7	16.27	0.1097	6.75	3	yes
PRD349	19 52 57.49	-51 58 17.1	17.91	0.1055	8.31	3	yes
PRD350	19 52 9.52	-52 03 39.9	17.39	0.1056	4.13	4	yes
PRD351	19 53 0.70	-52 01 14.3	17.79	0.1087	7.51	3	yes
PRD352	19 53 1.00	-51 48 35.3	17.60	0.1124	6.96	4	yes
PRD353	19 53 12.41	-52 06 31.6	16.91	0.1040	9.54	4	yes
PRD354	19 53 16.66	-51 47 38.5	18.71	-0.0002	8.33	4	
PRD355	19 53 22.60	-52 13 30.0	16.52	0.1087	3.83	4	yes
PRD356	19 53 2.80	-51 42 40.8	18.83	0.1053	6.36	3	yes
PRD357	19 53 29.80	-52 16 22.2	17.02	0.1093	6.01	3	yes
PRD358	19 53 33.09	-51 58 33.1	17.81	0.1083	6.37	4	yes
PRD359	19 53 35.99	-51 57 45.1	17.99	0.1010	3.39	4	yes
PRD360	19 53 36.55	-52 02 35.9	17.81	0.0499	3.68	4	
PRD361	19 53 3.89	-52 25 36.5	18.44	0.1897	8.70	3	
PRD362	19 53 40.31	-52 04 7.7	17.88	0.1125	6.16	3	yes
PRD363	19 53 40.64	-52 29 22.6	18.44	0.1898	5.08	4	
PRD364	19 53 42.77	-52 06 60.0	17.29	0.1072	6.64	3	yes
PRD365	19 53 4.63	-51 52 9.3	17.47	0.1065	3.05	4	yes
PRD366	19 53 55.88	-52 05 19.4	16.41	0.1045	7.20	3	yes
PRD367	19 53 8.19	-51 35 29.9	16.29	0.0000	10.63	4	
PRD368	19 53 9.43	-52 11 12.0	16.77	0.1107	6.81	3	yes
PRD369	19 54 19.84	-52 21 37.8	17.22	0.1093	6.32	3	yes
PRD370	19 54 19.91	-51 49 4.0	17.36	0.0876	3.41	4	
PRD371	19 54 22.38	-52 00 24.5	16.69	0.1008	4.79	4	yes
PRD372	19 54 30.71	-52 09 13.4	16.54	0.1062	7.54	3	yes
PRD373	19 54 35.35	-52 16 0.9	18.34	0.1075	5.83	3	yes
PRD374	19 54 3.95	-51 47 4.9	16.99	-0.0001	4.69	3	
PRD375	19 54 42.34	-51 35 58.0	17.84	-0.0002	9.01	4	

Table 3. continued.

Identification Tag	RA (J2000)	Dec (J2000)	R	z	TDV	Quality	Abell 3653 Member?
PRD376	19 54 45.01	-52 13 43.4	18.38	0.1458	5.20	4	
PRD377	19 54 47.49	-52 11 54.9	17.09	0.1092	6.40	4	yes
PRD378	19 54 57.52	-51 41 25.9	17.02	-0.0005	5.58	3	
PRD379	19 54 5.85	-51 50 44.4	18.21	0.0507	3.45	4	
PRD380	19 54 7.20	-51 47 34.6	19.06	0.1149	5.52	4	yes
PRD381	19 55 17.08	-51 37 32.2	17.15	0.0580	4.32	3	
PRD382	19 55 2.04	-52 24 42.4	16.87	0.0573	6.22	3	
PRD383	19 55 27.09	-51 58 53.0	18.46	0.1558	8.32	3	
PRD384	19 55 31.27	-52 28 3.7	17.81	0.0002	6.72	4	
PRD385	19 55 32.27	-51 38 14.6	17.42	0.0868	5.96	3	
PRD386	19 55 32.72	-52 17 16.4	18.67	0.1997	7.64	3	
PRD387	19 55 38.38	-51 57 4.7	18.45	0.2279	5.46	4	
PRD388	19 55 41.62	-51 39 20.8	17.88	0.0880	3.30	4	
PRD389	19 55 41.65	-52 14 49.3	18.46	0.0995	2.75	4	yes
PRD390	19 55 50.90	-52 29 52.1	16.63	0.0499	2.90	4	
PRD391	19 55 52.54	-52 03 8.9	16.92	0.1078	6.03	3	yes